ISSN 1028-334X, Doklady Earth Sciences, 2020, Vol. 495, Part 1, pp. 821–826. © Pleiades Publishing, Ltd., 2020.
Russian Text © The Author(s), 2020, published in Doklady Rossiiskoi Akademii Nauk. Nauki o Zemle, 2020, Vol. 495, No. 1, pp. 25–30.

MINERALOGY

"Invisible" Gold in Pyrite and Arsenopyrite from the Pavlik Deposit (Northeastern Russia)

N. V. Sidorova[a,*], V. V. Aristov[a,], A. V. Grigor'eva[a], and Corresponding Member of the RAS A. A. Sidorov[a]**

Received August 4, 2020; revised August 26, 2020; accepted September 1, 2020

Abstract—The first study on the distribution pattern and features of the "invisible" gold concentration in pyrite and arsenopyrite was carried out for a typical gold–quartz deposit of the Kolyma region. It was established that the main concentrator of "invisible" gold on the Pavlik deposit is the Late Arsenian pyrite-2. The method of Laser Ablation-Inductivity Coupled Plasma-Mass Spectrometer (LA-ICP-MS) gives an Au content up to 478 g/t; the Electron Microprobe Analysis (EMPA) gives up to 570 g/t by. The As content, determined by LA-ICP-MS is up to 4.1 wt % and up to 3.4 wt % by EMPA. Pyrite-2 overgrows and replaces the early pyrite-1 with a reduced content of As and Au. Microinclusions of the Pb–Zn–Cu–Sb–Ag–Bi–containing phases are concentrated at the boundaries of the pyrite-1 and pyrite-2 blocks. Pyrite-2 is depleted by an order in Cu, Zn, Ag, Sb, Pb, and Bi in comparison with pyrite-1. The max Au/As molar ratio in pyrite-2 is 0.006, which suggests the presence of Au in the form of a solid solution. In another case, pyrite, depleted by trace elements, is cemented with As, Ag, Sb, Au, and Pb-rich marcasite with native gold. In arsenopyrite, there is a homogeneous distribution of gold at low concentrations (up to 3 g/t) in euhedral crystals and a heterogeneous distribution (up to 7 g/t) in deformed fissured grains.

Keywords: Russian Northeast, Pavlik gold deposit, pyrite, arsenopyrite, "invisible" gold, EMPA, LA-ICP-MS

DOI: 10.1134/S1028334X20110136

Many works have been dedicated to the problem of "invisible" fine-grained gold, which is disseminated in pyrite and arsenopyrite of hygrothermal gold ore deposits [1–6]. Determination of the concentrations and distribution patterns of gold and other microelements in ore minerals of the deposits has become widespread due to the development and wide use of the precision analyses of mineral matter. Currently, the method of X-ray Absorption Spectroscopy (XAS) is thriving. This method provides accurate information about the gold deportment in minerals of the Fe–As–S system [7, 8].

This paper reports new data on the microelement composition and distribution patterns of gold in pyrite and arsenopyrite of the Pavlik deposit. These studies allow us to clarify the conceptions relating to the ore formation of the large gold–quartz deposits of the Yana–Kolyma gold ore province and may contribute to optimization of the extraction of useful components from ores.

The Pavlik deposit is situated in the Omchak ore-placer cluster of Magadan oblast. The ore field is composed of Upper Permian volcanic–sedimentary rocks, folded in the near-fault folds. On the flanks of the deposit, there are small intrusions with intermediate and felsic composition [9].

The main type of ore bodies is mineralized crush zones, which were formed due to hydrothermal processes and repeated tectonic impacts. Within the ore zones, there are boudines of dikes with an intermediate (diorite–porphyrites), more rarely, felsic (rhyolite, quartz porphyries) composition, as well as quartz veins and tectonic and hydrothermal breccia, and cemented by quartz and quartz carbonate. The content of sulfides in ores is about 1%. Pyrite and arsenopyrite are mostly disseminated in host rocks, quartz–carbonate cement, and vein quartz in the form of impregnations and grain intergrowths. The average content of Au in the ores is about 3 g/t. Most of the Au is represented by microscopical native gold (the grain size peak is 0.075 mm) [10].

[a] *Institute of Geology of Ore Deposits, Petrography, Mineralogy, and Geochemistry, Russian Academy of Sciences, Moscow, 119017 Russia*

**e-mail: nsidorova989@mail.ru*

***e-mail: rstvvv@yandex.ru*

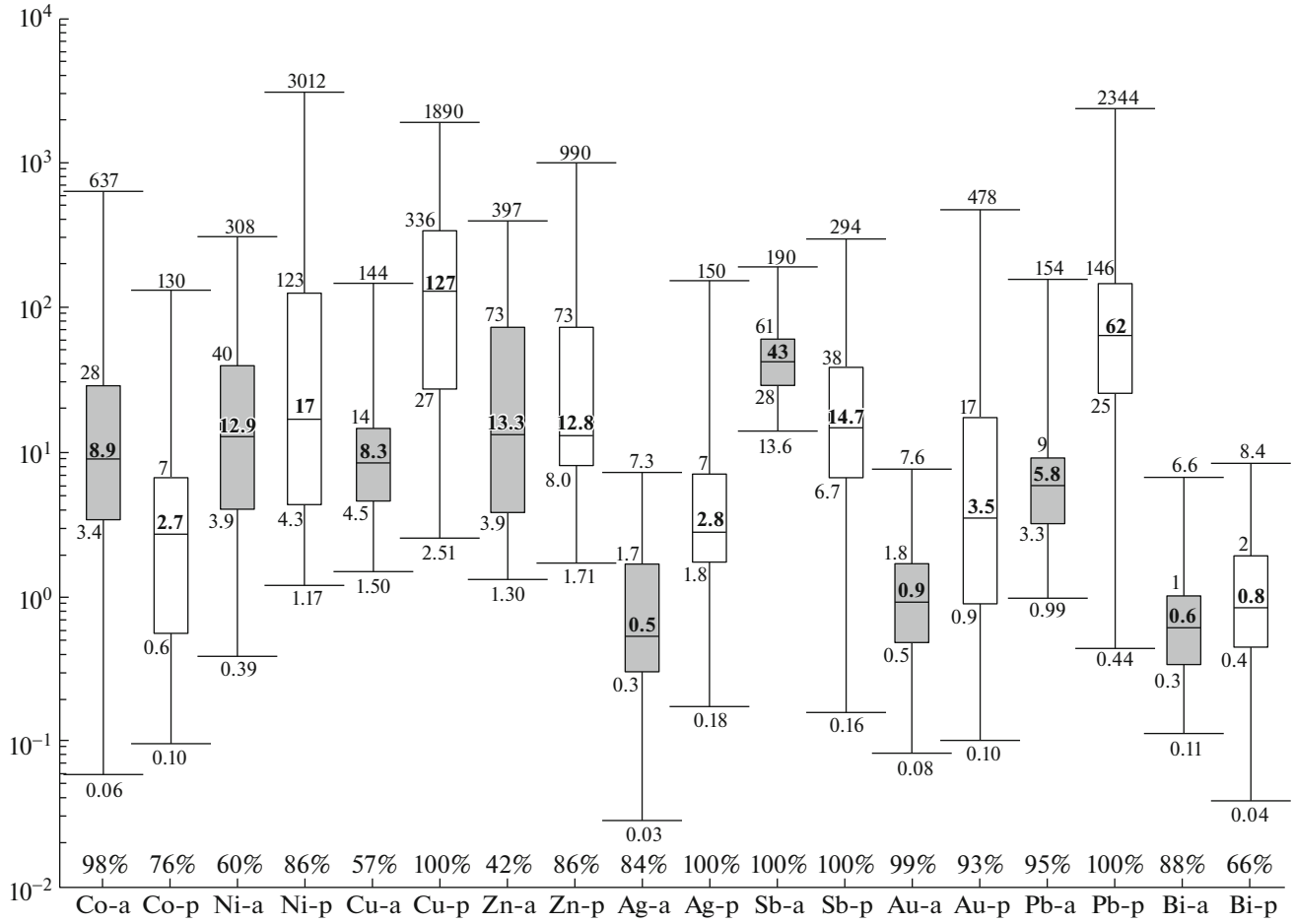

Fig. 1. The box plot of the content of trace microelements in (a) arsenopyrite and (p) pyrite of the Pavlik deposit. The boundaries of the "box" are the first and third quartiles, and the line in the middle of the "box" is the median. The frequency of occurrence of the component (%) is shown above the X-axis. The values of the concentrations (g/t) are on the Y-axis.

To study the gold mineralization of sulfides from the ore zones, ten samples with an Au content from 6 to 14 g/t were taken. Monofractions of pyrite and arsenopyrite were selected from these samples. The ores are represented by breccia with debris of silty stones, which are cemented by a sericite–ankerite–quartz–albite aggregate. Arsenopyrite predominated (80–96% of sulfide mineralization) in most of the samples. An approximately equal amount of arsenopyrite and pyrite was established in several samples. The selected grains of arsenopyrite are euhedral with short-prismatic or long-columnar habitus up to 1.5–2 mm across (on average, 0.5 mm). The selected grains of pyrite are anhedral with crystallographic outlines.

The chemical composition of the sulfides studied was determined with the use of a JXA-8200 ("JEOL") X-ray spectral analyzer (method of X-ray Spectrum Microanalysis, laboratory of the Institute of Geology of Ore Deposits, Petrography, Mineralogy, and Geochemistry, Russian Academy of Science, analyst E.V. Koval'chuk). The Au content (detection limit (3σ) 45 ppm) was measured in sulfides according to the method described thoroughly in [4]. The separate grains of sulfides were analyzed on an XSeries quadrupole spectrometer, equipped with the NewWave UP-213 accessory for laser sampling with a laser ray of 30–80 μm in diameter (LA-ICP-MS method, laboratory of the Institute of Geology of Ore Deposits, Petrography, Mineralogy, and Geochemistry, Russian Academy of Science, analyst V.D. Abramova). The parameters of ablation and the method of data processing are published in [11]. Using the laser accessory, 26 spot samples and seven profile samples were taken from 33 grains of pyrite and 29 spot samples and 22 profile samples were taken from 51 grains of arsenopyrite.

As a result of microscopical studies, it has been established that metacrystals of pyrite are mutually intergrown with arsenopyrite, more rarely, with sphalerite (Fig. 2); they contain relicts of host rocks and small inclusions of monazite, rutile, galena, and sphalerite. Pyrite is crushed here and there and partially replaced and cemented by marcasite; at the boundary of these minerals, native gold is encountered (Fig. 3).

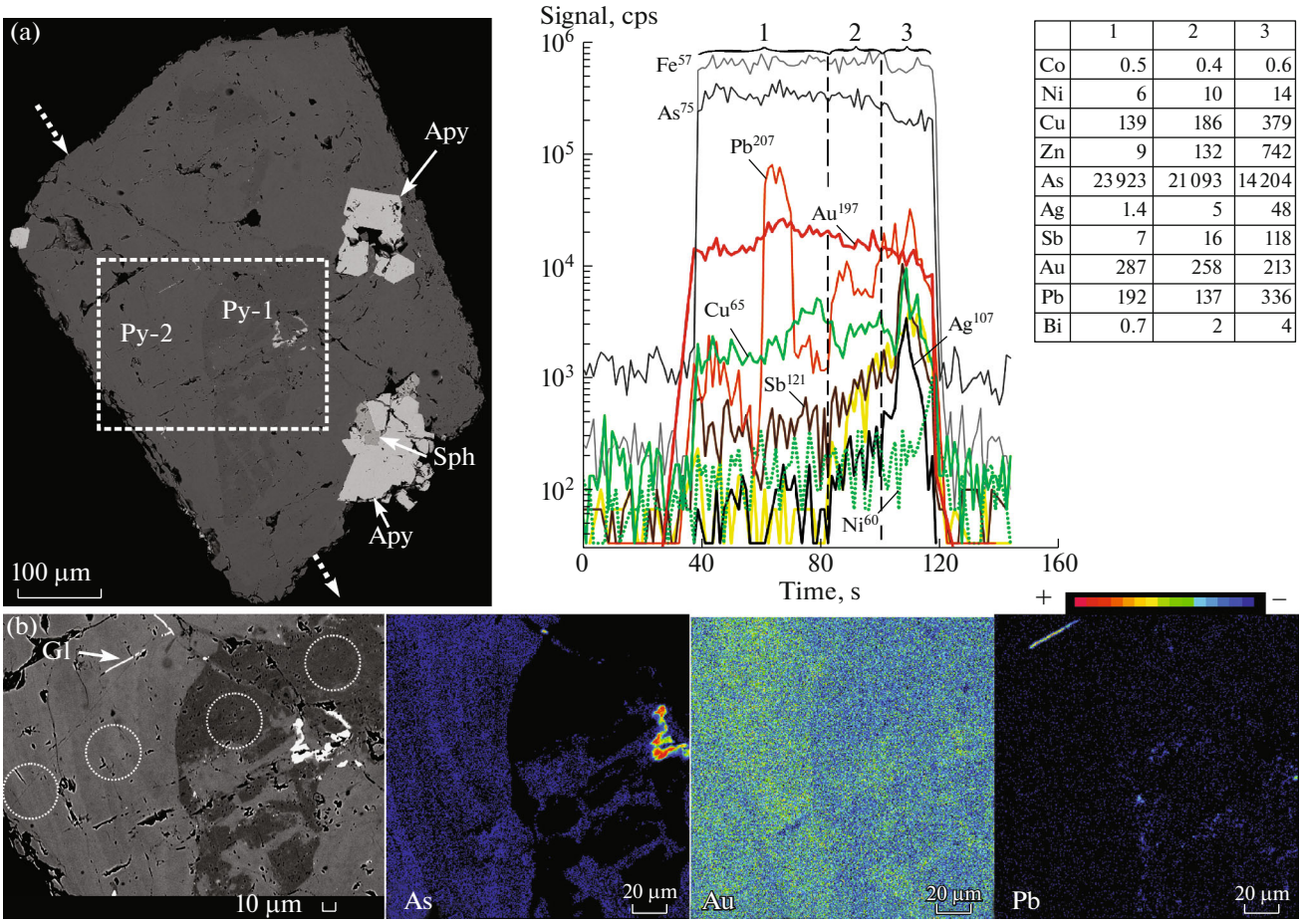

	1	2	3
Co	0.5	0.4	0.6
Ni	6	10	14
Cu	139	186	379
Zn	9	132	742
As	23923	21093	14204
Ag	1.4	5	48
Sb	7	16	118
Au	287	258	213
Pb	192	137	336
Bi	0.7	2	4

Fig. 2. The metacrystal of pyrite, intergrown with arsenopyrite (Apy) and sphalerite (Sph), and veinlets and inclusions of galena (Gl): (a) general view, in the dash–line square, the field, which is enlarged in Fig. 2b, is illustrated; the arrows point to the location and direction of the ablation profile, which is shown to the right with the average values of the components (g/t) in the distinguished intervals; (b) the fragment of the pyrite grain (points of ablation are shown by the dash–line circles) with the element distribution maps, obtained by EMPA: As (Lα, TAP), Au (Mα, PETH), Pb (Mα, PETH); current 20 nA, time at a point is 60 ms.

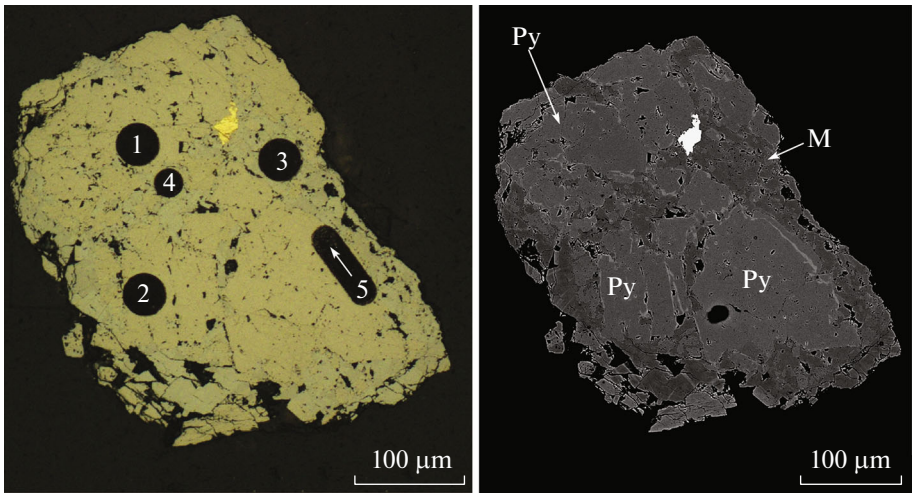

Fig. 3. The breccia-like intergrowths of pyrite (Py) and marcasite (M) with native gold (the brightest phase). To the left, the image is represented in the reflected light in the optical microscope with ablation craters; to the right, it is represented in back-scattered electrons.

Table 1. The composition of pyrite (Py) and marcasite (M) (g/t) according to the LA–ICP–MS data. Numbers of samples correspond to the numbers in Fig. 3

No.	Co	Ni	Cu	Zn	As	Ag	Sb	Au	Pb	Bi
1-Py	–	–	380	384	550	2.6	11.9	3.8	81.9	–
2-Py	–	3.1	17.8	11.8	117	1.9	7	0.9	70.2	–
3-M	1.4	12.3	90	6.8	3980	53.2	191	6.7	443	1.1
4-M	–	–	52	35	3450	38.8	92	12.9	439	–
5-LINE	–	–	78	–	8610	4.6	37.6	51.8	178	–

According to EMPA the formula of pyrite is $Fe_{0.98–1.01}As_{0–0.06}S_{1.94–2.01}$; in 22% of all analytical points (36), the As concentration is lower than the detection limit (<0.06 wt %); Co was established (≥0.06 wt %) in 36% analyses and its content went up to 0.08 wt %. Au in pyrite is established in 36% of all analyses.

The composition of arsenopyrite is

$$Fe_{1.02–1.03}As_{0.88–0.98}S_{1.00–1.09}.$$

In 30% of all analytical points (59), the Co concentration is 0.06–0.14 wt %. Au in arsenopyrite is established in 27% analyses, and its content goes up to 70 g/t (in a single case); generally, it is 40–50 g/t. The scanning of the cuts of arsenopyrite grains in the backscattered electrons (BSE) revealed poor zoning with a decrease in the As concentration and an increase in S toward the edges of the crystals and a barely visible sectoral heterogeneity for Co.

The contents of microelements obtained by the LA-ICP-MS method were divided into three groups in accordance with the selections where the component concentration is higher than the detection limit:

(1) 80–100% is commonly found trace elements: Co, Ag, Sb, Au, and Pb for both sulfides (Fig. 1), including Bi for arsenopyrite and Ni, Cu, and Zn for pyrite;

(2) 40–80% is for Ni, Cu, and Zn, which are trace elements for arsenopyrite; Mn, Ga, Ge, and Tl, for pyrite; and

(3) <40% is for Cd, In, Sn, and Te for both sulfides, and Mn, Ga, Ge, and Tl for arsenopyrite.

These elements are included into the composition of microinclusions of other minerals; their content rarely exceeds 6 g/t, and, usually, is 0.0n–0.n g/t. An exception is Mn: in pyrite, its content goes up to 643 g/t, and in arsenopyrite, to 266 g/t.

Arsenian pyrite with an increased gold content (C_{Au} > avg. geom. = 4.2 g/t) has been thoroughly studied. One metacrystal with the highest concentration of Au was studied with the use of selective mapping in the characteristic spectrums (Fig. 2). On the image in backscattered electrons, in pyrite, there are dark fields with a decreased content of As (up to 0.4 wt %) and Au (up to 0.007 wt %) and light fields, where the amount of As goes up to 3.4 wt % and the Au content ranges from 140 to 570 g/t with a tendency toward an increase in Au (and As) toward the grain edge (Figs. 2a, 2b). On the distribution map (Fig. 2b As), the dark fields reflect low-arsenian pyrite-1, while the white spot is the grain of arsenopyrite. In the left-hand side of Fig. 2b As, there are the distinct ark-shaped fields of a lighter color, which are enriched in arsenic; they are subparallel to the clearly manifested boundary between pyrite-1 and arsenian pyrite-2. The gold-rich zones coincide well with the fields with increased contents of arsenic (Fig. 2b Au). Pb is concentrated in the form of mineral phase-microinclusions along the blocks of pyrite-1 and pyrite-2 (Fig. 2b Pb).

In the spot samples of ablation (with a laser ray of 40 μm in diameter, Fig. 2b), the contents (in g/t, values are recalculated from the center to the edge of a grain) of Cu (317–266), Zn (990–528), As (4480–11100), Ag (14.7–13.5), Sb (85–79), Au (30–88), Pb (318–953), and Bi (1.2–3.8) were established in pyrite-1. In pyrite-2, the content of all elements, except As and Au, is an order of magnitude less than in pyrite-1, and their amount decreases toward the center of the grain; in the outermost point of ablation, the concentrations (in g/t) of Cu, 88; Zn < 6; As, 41 900; Ag, 0.9; Sb, 4; Au, 418; Pb, 23; and Bi, 0.07.

In the aggregates from pyrite blocks, which are cemented by marcasite (Fig. 3), thin (1–4 μm) rims, enriched in As and Au, are encountered. Table 1 shows that marcasite is significantly enriched in As, Ag, Sb, and Pb in comparison with pyrite; increased contents of microelements in pyrite are noted only at one point for Cu and Zn. Hence, the amount of As and Au increases in the light (in BSE-regime) rims in pyrite (Table 1, 5-LINE analysis), which demonstrates the selective concentration of these elements at the boundary of the pyrite and marcasite blocks.

In arsenopyrite, the sounding profiles were generally made for the cuts of euhedral grains. Sb is homogenously distributed along the profile with sufficiently persistent contents; the Co distribution is rhythmi-

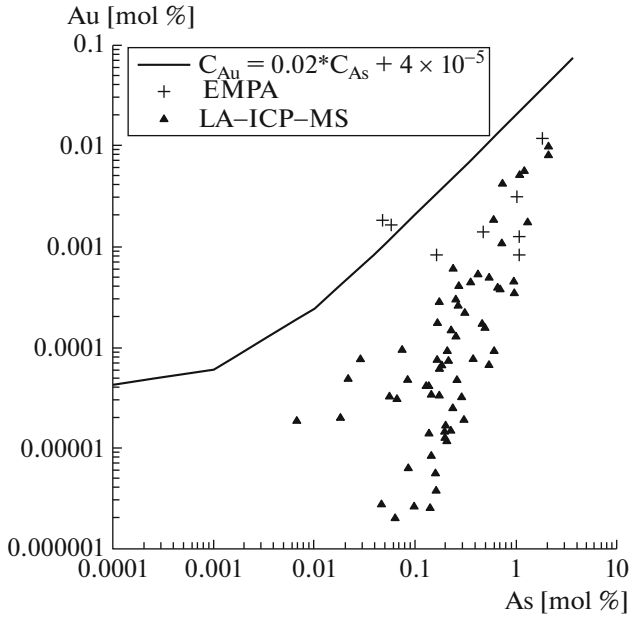

Fig. 4. The plot of the Au–As concentrations (mol %) of the Pavlik deposit. The assumed limit of the gold solubility is shown by a solid line [6].

cally zonal with a tendency to increase from the center to the edges of the crystal; Ag gives discrete peaks at contents up to 2 g/t and a heterogenous distribution along the entire profile at contents of 2–7 g/t, together with Bi, Pb, and, more rarely Au. Pb is characterized by a homogenous distribution and small peaks together with Ag, Bi, Te, less often, Co and Ni. The homogenous distribution of gold predominates in euhedral crystals at a content of up to 3 g/t, and a heterogenous distribution is common for fissured and deformed grains at contents of 5–7 g/t, together with Cu, Zn, Ag, and Bi.

DISCUSSION

When plotting all compositions of pyrite on the As–Au plot [6], most of the samples occurred below the line reflecting an empirical limit of solubility of gold in pyrite (Fig. 4). Two samples of low-arsenian pyrite-1 fall above the line. Three samples (EMPA) are characterized by an As content that is lower than the detection limit (0.02 and 0.04 wt %). Two of them are from pyrite-1, and one is from pyrite intergrown with marcasite; the Au content for them is 60, 70, and 90 g/t. When the As detection limit decreases to 0.02 wt % (1σ), these samples will occur above the line too. According to [6], below this line, gold was in the form of a solid solution in pyrite; it was sorbed from solutions nonsaturated by Au, where gold was in the form of hydrosulfide complexes [12]. However, above the line, gold presents in pyrite in the form of nanosized particles. According to [7, 8], Au may occur in the condition of the solid solution in As-depleted pyrite. Taking into consideration the EMPA data, in low-arsenian pyrite of the Pavlik deposit, the gold, the content of which is higher than the detection limit, is sparsely distributed, and according to LA-ICP-MS data, the Au distribution is associated with Ag. This may give evidence of submicron particles of Au^0.

The data obtained allow us to reconstruct partially the process of interaction of the fluids from which sulfides and gold were deposited. At the initial stage of gold deposition from the solution, which is nonsaturated in relation to Au, thin rims of As-pyrite with Au^{+1} were developed in the depleted pyrite under increased temperatures during the relatively quick deposition. Further, in the saturation of the solution, these rims were overgrown by marcasite with native gold.

Pyrite-1 with submicron Au^0, together with arsenopyrite, apparently, served as a "seed" in the crystallization of arsenian gold-bearing pyrite from the residual solutions nonsaturated with gold during the late process. This ratio of the late gold-bearing pyrite to the early one dramatically differs from the ratio that was established on the Sukhoi Log deposit [2], and is close to the ratio of the Au, As-rich pyrite to the pure pyrite of the Carlin-type deposits and sulfide deposits of the Urals [3, 5].

CONCLUSIONS

Therefore, the range of the concentrations and distribution pattern of "invisible" gold for pyrite and arsenopyrite of the Pavlik deposit were determined for the first time.

It was established that (1) the basic mineral-concentrator of "invisible" gold is arsenian pyrite, (2) FeS_2-phases on the deposit are represented by the trace element-depleted pyrite (1) in association with the As, Pb, Ag, and Sb-rich marcasite and native gold, and by the Late Arsenian gold-bearing pyrite (3), (3) in arsenopyrite, low concentrations and a homogenous distribution of Au are common for euhedral crystals, and a heterogenous distribution is common for deformed crystals.

Native gold with trace minerals is deposited in microfissures of sulfides and host rocks at a mostly independent stage of mineral formation.

FUNDING

This work was carried out according to a State Assignment of the Institute of Geology of Ore Deposits, Petrography, Mineralogy, and Geochemistry, Russian Academy of Sciences, "Metallogeny of the Ore Regions of the Volcano-Pluton-related and Folded Orogenic Belts of the Russian Northeast."

REFERENCES

1. A. D. Genkin, N. S. Bortnikov, L. J. Cabri, et al., Econ. Geol. **93**, 463–487 (1998).
2. R. R. Large, V. V. Maslenikov, F. Robert, et al., Econ. Geol. **102**, 1233–1267 (2007).
3. I. V. Vikentyev, Geol. Ore Deposits **57** (4), 237–266 (2015).
4. E. V. Kovalchuk, B. R. Tagirov, I. V. Vikentyev, et al., Geol. Ore Deposits **461** (5), 447–469 (2019).
5. P. Gopon, J. O. Douglas, M. A. Auger, et al., Econ. Geol. **114**, 1123–1133 (2019).
6. M. Reich, S. E. Kesler, S. Utsunomiya, et al., Geochim. Cosmochim. Acta **69**, 2781–2796 (2005).
7. A. L. Trigub, B. R. Tagirov, K. O. Kvashnina, et al., Am. Mineral. **102**, 1057–1065 (2017).
8. O. N. Filimonova, B. R. Tagirov, A. L. Trigub, et al., Ore Geol. Rev. **121**, 103475 (2020).
9. Yu. S. Savchuk, A. V. Volkov, V. V. Aristov, et al., Rudy Met., No. 2, 77–85 (2018).
10. V. V. Aristov, A. V. Grigor'eva, Yu. S. Savchuk, et al., Geol. Miner.-Syr'evye Resur. Sev.-Vostoka Ross. **1**, 18–21 (2018).
11. V. D. Abramova, Metallog. Drevnikh Sovrem. Okeanov, No. 1, 256–258 (2018).
12. G. Simon, S. E. Kesler, and S. L. Chryssoulis, Econ. Geol. **94**, 405–421 (1999).

Translated by V. Krutikova